

Synchrotron (Undulator / Wiggler) Radiation Simulation with SRW



O. Chubar, NSLS-II, BNL

Collaboration Meeting on "Simulation and Modeling for SR Sources and X-Ray Optics"

October 1 - 2, 2015, NSLS-II



BROOKHAVEN
NATIONAL LABORATORY
BROOKHAVEN SCIENCE ASSOCIATES

Emission by a Relativistic Charged Particle in Free Space: Retarded Potentials Approach

$$\vec{A} = e \int_{-\infty}^{+\infty} \vec{\beta}_e R^{-1} \delta(\tau - t + R/c) d\tau, \quad \varphi = e \int_{-\infty}^{+\infty} R^{-1} \delta(\tau - t + R/c) d\tau \quad (\text{Gaussian CGS})$$

$$\Downarrow \quad \delta(t') = (1/2\pi) \int_{-\infty}^{+\infty} \exp(i\omega t') d\omega$$

$$\vec{A} = \frac{e}{2\pi} \int_{-\infty}^{+\infty} \exp(-i\omega t) d\omega \int_{-\infty}^{+\infty} \vec{\beta}_e R^{-1} \exp[i\omega(\tau + R/c)] d\tau$$

$$\varphi = \frac{e}{2\pi} \int_{-\infty}^{+\infty} \exp(-i\omega t) d\omega \int_{-\infty}^{+\infty} R^{-1} \exp[i\omega(\tau + R/c)] d\tau$$

Ternov used this approach to derive far-field SR expressions

$$\vec{E} = -\frac{1}{c} \frac{\partial \vec{A}}{\partial t} - \nabla \varphi = \frac{ie}{2\pi c} \int_{-\infty}^{+\infty} \omega \cdot \exp(-i\omega t) d\omega \int_{-\infty}^{+\infty} [\vec{\beta}_e - [1 + ic/(\omega R)] \cdot \vec{n}] R^{-1} \exp[i\omega(\tau + R/c)] d\tau$$

$$\Downarrow \quad \vec{E}_\omega \equiv \int_{-\infty}^{+\infty} \vec{E} \exp(i\omega t) dt$$

Exact expression, valid in the Near Field:

$$\vec{E}_\omega = iec^{-1} \omega \int_{-\infty}^{+\infty} [\vec{\beta}_e - [1 + ic/(\omega R)] \cdot \vec{n}] R^{-1} \exp[i\omega(\tau + R/c)] d\tau \quad (\checkmark)$$

The equivalence of (✓) to the well-known expression of Jackson can be shown by integration by parts

$$\vec{E}_\omega = ec^{-1} \int_{-\infty}^{+\infty} \frac{\vec{n} \times [(\vec{n} - \vec{\beta}_e) \times \dot{\vec{\beta}}_e] + cR^{-1} \gamma^{-2} (\vec{n} - \vec{\beta}_e)}{R \cdot (1 - \vec{n} \cdot \vec{\beta}_e)^2} \cdot \exp[i\omega(\tau + R/c)] d\tau$$

Emission by a Relativistic Charged Particle Efficient Computation

Exact expression obtained from Retarded Potentials:

$$\vec{E}_\omega = iec^{-1}\omega \int_{-\infty}^{+\infty} [\vec{\beta}_e - [1 + ic/(\omega R)] \cdot \vec{n}] R^{-1} \exp[i\omega(\tau + R/c)] d\tau$$

Phase expansion valid in the Near Field:

$$\omega \cdot (\tau + R/c) \approx \Phi_0 + \frac{\pi}{\lambda} \left[s\gamma^{-2} + \int_0^s |\vec{\beta}_{e\perp}|^2 d\tilde{s} + \frac{(x-x_e)^2 + (y-y_e)^2}{z-s} \right]$$

Particle dynamics in external magnetic field:

$$\vec{r}_e = \vec{r}_e(s, \vec{r}_{e0}, \vec{\beta}_{e0}); \quad \vec{\beta}_e \approx d\vec{r}_e/ds$$

Asymptotic expansion of the radiation integral (to accelerate computation):

$$\int_{-\infty}^{+\infty} F \exp(i\Phi) ds = \int_{s_1}^{s_2} F \exp(i\Phi) ds + \int_{-\infty}^{s_1} F \exp(i\Phi) ds + \int_{s_2}^{+\infty} F \exp(i\Phi) ds$$

$$\int_{-\infty}^{s_1} F \exp(i\Phi) ds + \int_{s_2}^{+\infty} F \exp(i\Phi) ds \approx \left[\left(\frac{F}{i\Phi'} + \frac{F'\Phi' - F\Phi''}{\Phi'^3} + \dots \right) \exp(i\Phi) \right]_{s_2}^{s_1}$$

Temporally-Incoherent and Coherent Spontaneous Emission by Many Electrons

Electron Dynamics:

$$\begin{pmatrix} x_e \\ y_e \\ z_e \\ \beta_{xe} \\ \beta_{ye} \\ \delta\gamma_e \end{pmatrix} = \mathbf{A}(\tau) \begin{pmatrix} x_{e0} \\ y_{e0} \\ z_{e0} \\ x'_{e0} \\ y'_{e0} \\ \delta\gamma_{e0} \end{pmatrix} + \mathbf{B}(\tau) \quad \leftarrow \text{Initial Conditions}$$

Spectral Photon Flux per unit Surface emitted by the **whole Electron Beam:**

$$\frac{dN_{ph}}{dtdS(d\omega/\omega)} = \frac{c^2 \alpha I}{4\pi^2 e^3} \langle |\vec{E}_\omega|^2 \rangle$$

"Incoherent" SR

$$\langle |\vec{E}_\omega|^2 \rangle = \int \left| \vec{E}_{\omega 0}(\vec{r}; x_{e0}, y_{e0}, z_{e0}, x'_{e0}, y'_{e0}, \delta\gamma_{e0}) \right|^2 f(x_{e0}, y_{e0}, z_{e0}, x'_{e0}, y'_{e0}, \delta\gamma_{e0}) dx_{e0} dy_{e0} dz_{e0} dx'_{e0} dy'_{e0} d\delta\gamma_{e0} +$$

$$+ (N_e - 1) \left| \int \vec{E}_{\omega 0}(\vec{r}; x_{e0}, y_{e0}, z_{e0}, x'_{e0}, y'_{e0}, \delta\gamma_{e0}) f(x_{e0}, y_{e0}, z_{e0}, x'_{e0}, y'_{e0}, \delta\gamma_{e0}) dx_{e0} dy_{e0} dz_{e0} dx'_{e0} dy'_{e0} d\delta\gamma_{e0} \right|^2$$

Coherent SR

Common Approximation for CSR: "Thin" Electron Beam: $\langle |\vec{E}_\omega|^2 \rangle_{CSR} \approx N_e \left| \int_{-\infty}^{\infty} \tilde{f}(z_{e0}) \exp(ikz_{e0}) dz_{e0} \right|^2 |\vec{E}_{\omega 1}|^2$

For Gaussian Longitudinal Bunch Profile: $\langle |\vec{E}_\omega|^2 \rangle_{CSR} \approx N_e \exp(-k^2 \sigma_b^2) |\vec{E}_{\omega 1}|^2$

If $f(x_{e0}, y_{e0}, z_{e0}, x'_{e0}, y'_{e0}, \delta\gamma_{e0})$ is Gaussian, 6-fold integration over electron phase space can be done analytically for the (Mutual) Intensity of Incoherent SR and for the Electric Field of CSR

Self-Amplified Spontaneous Emission Described by Paraxial FEL Equations

Approximation of Slowly Varying Amplitude of Radiation Field

Particles' dynamics
in undulator and radiation fields
(averaged over many periods):

$$\frac{d\theta}{dz} = k_u - k_r \frac{1 + p_{\perp}^2 + a_u^2 - 2a_r a_u \cos(\theta + \phi_r)}{2\gamma^2}$$

$$\frac{d\gamma}{dz} = -\frac{k_r f_c a_r a_u}{\gamma} \sin(\theta + \phi_r)$$

$$\frac{d\vec{p}_{\perp}}{dz} = -\frac{1}{2\gamma} \frac{\partial a_u^2}{\partial \vec{r}_{\perp}} + \mathbf{k}_{foc} \vec{r}_{\perp}$$

$$\frac{d\vec{r}_{\perp}}{dz} = \frac{\vec{p}_{\perp}}{\gamma}$$

Paraxial wave equation
with current:

$$\left[2ik_r \frac{\partial}{\partial z} + \nabla_{\perp}^2 \right] a_r \exp(i\phi_r) = -\frac{e\varepsilon_0 I f_c a_u}{mc} \left\langle \frac{\exp(-i\theta)}{\gamma} \right\rangle$$

W.B.Colson
J.B.Murphy
C.Pellegrini
E.Saldin
E.Bessonov
et. al.

Solving this system gives Electric Field at the FEL exit for one "Slice": $E_{slice}|_{z=z_{exit}} \sim a_r \exp(i\phi_r)|_{z=z_{exit}}$

Loop on "Slices" (copying Electric Field to a next slice from previous slice, starting from back)

Popular TD 3D FEL computer code: **GENESIS** (S.Reiche)

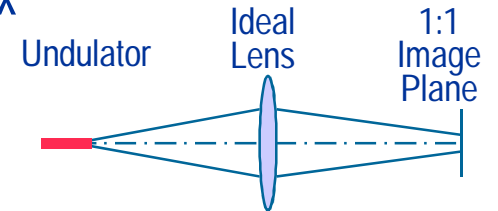
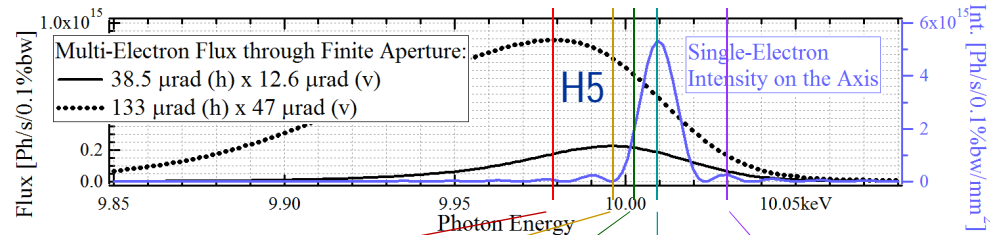
One run provides Time-Domain Electric Field in transverse plane at FEL exit: $E(x, y, z_{exit}, t)$

Electric Field in **Frequency** domain: $\vec{E}(\vec{r}, \omega) \equiv \int_{-\infty}^{\infty} \vec{E}(\vec{r}, t) \exp(i\omega t) dt$

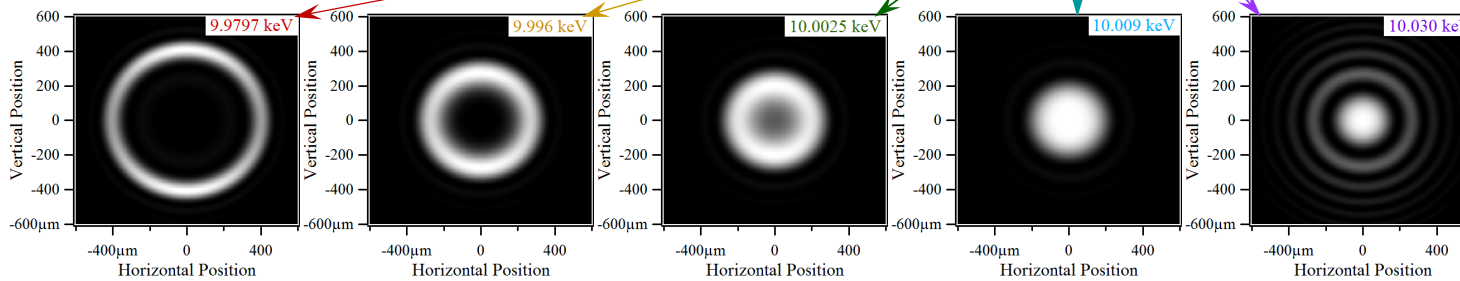
Single-Electron (Fully Transversely-Coherent) UR Intensity Distributions "in Far Field" and "at Source"

UR "Single-Electron" Intensity and "Multi-Electron" Flux

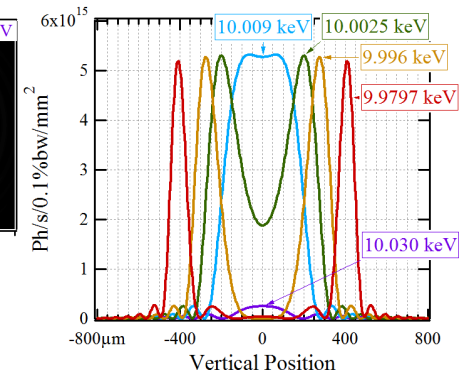
E-Beam Energy: 3 GeV
 Current: 0.5 A
 Undulator Period: 20 mm



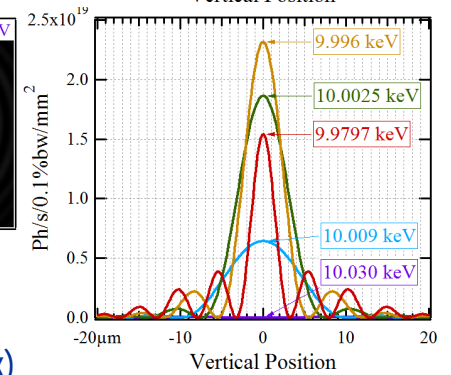
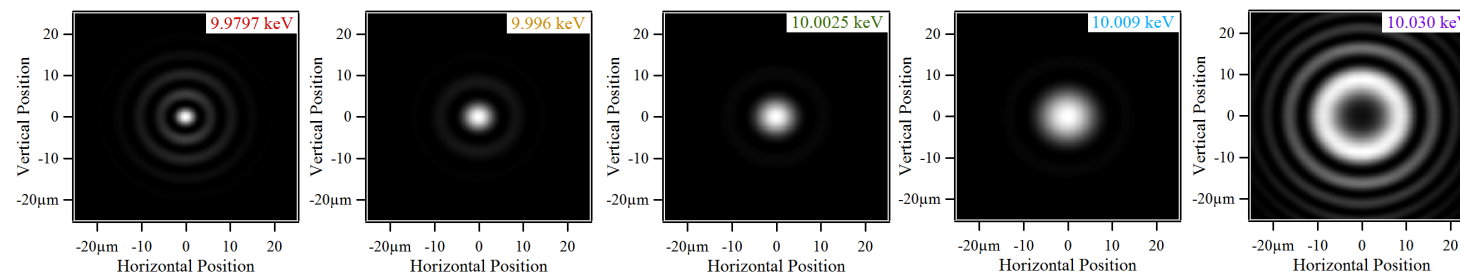
Intensity Distributions at 30 m from Undulator Center



Vertical Cuts (x = 0)



Intensity Distributions in 1:1 Image Plane



"Phase-Space Volume" Estimation for Vertical Plane

(RMS sizes/divergences calculated for the portions of intensity distributions containing 95% of flux)

$$\sigma_y \sigma_y' \approx 7.7 \frac{\lambda}{4\pi}$$

$$3.3 \frac{\lambda}{4\pi}$$

$$1.9 \frac{\lambda}{4\pi}$$

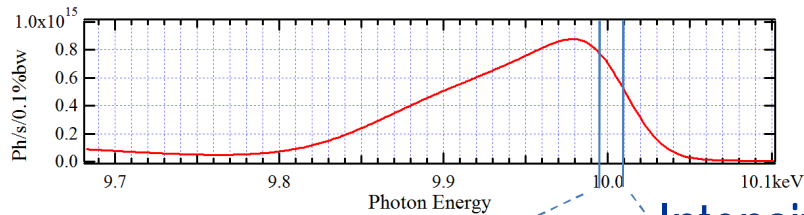
$$1.5 \frac{\lambda}{4\pi}$$

$$9.2 \frac{\lambda}{4\pi}$$

Estimation of X-Ray Beam Angular Divergence and Source Size by Wavefront Propagation

IVU20-3m Spectral Flux

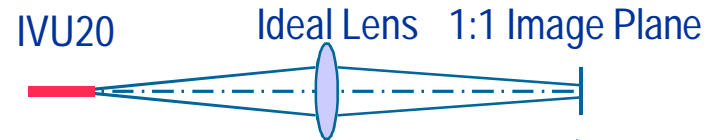
through 100 μm (H) x 50 μm (V) Aperture at K~1.5 providing H5 peak at ~10 keV



Electron Beam:

Hor. Emittance: 0.9 nm
Vert. Emittance: 8 pm
Energy Spread: 8.9×10^{-4}
Current: 0.5 A
Low-Beta Straight

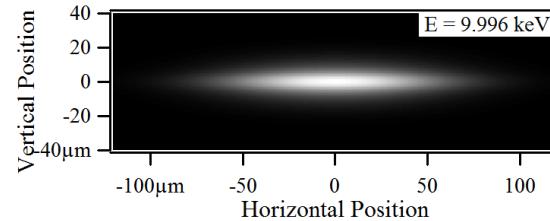
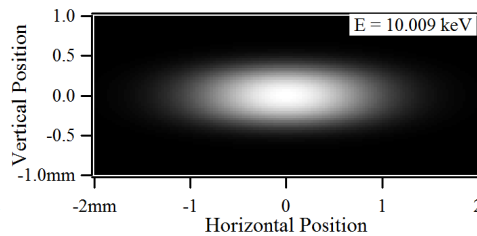
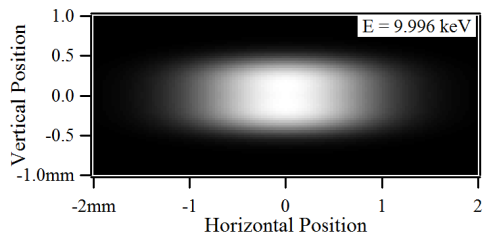
Test Optical Scheme



Intensity Distributions at ~10 keV

At 30-m from Undulator

In 1:1 Image Plane

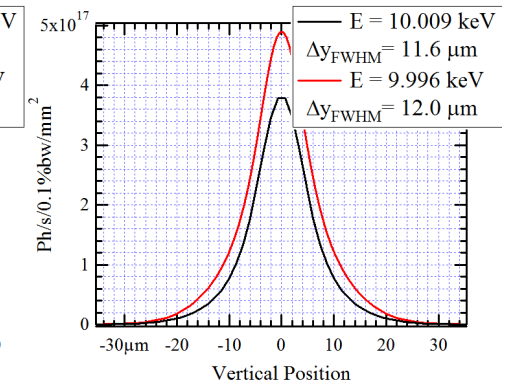
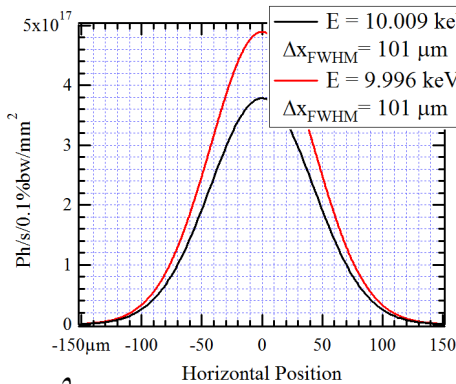
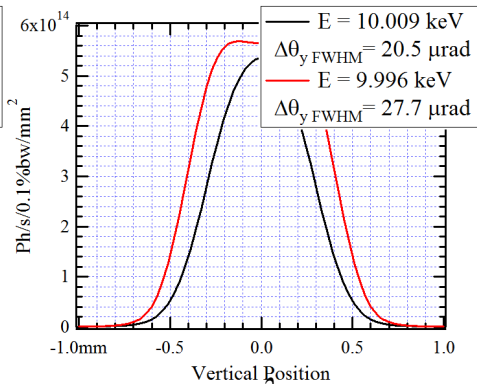
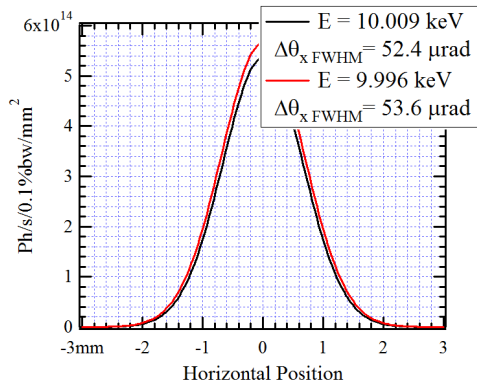


Horizontal Cuts (y = 0)

Vertical Cuts (x = 0)

Horizontal Cuts (y = 0)

Vertical Cuts (x = 0)



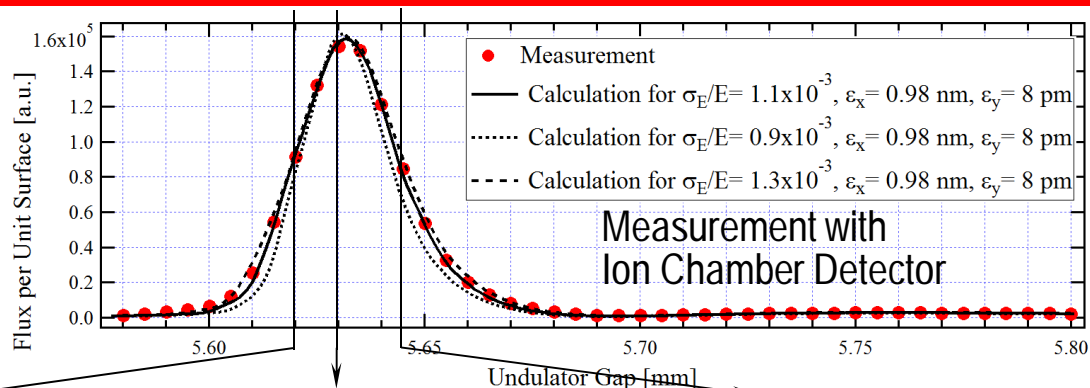
$$\sigma_x \sigma_x' \approx 97 \frac{\lambda}{4\pi}; \quad \sigma_y \sigma_y' \approx 5.7 \frac{\lambda}{4\pi}$$

...very far from Coherent Gaussian Beam!

On-Axis "Gap Spectrum" and Intensity Distributions of Radiation from IVU20 at HXN Beamline (I)

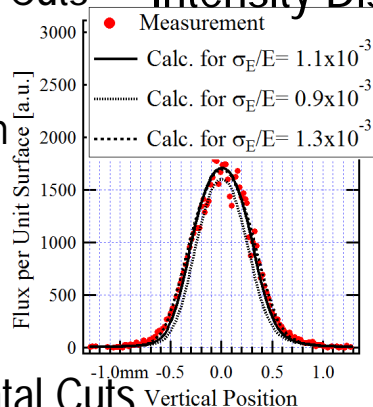
On-Axis Gap Spectrum at ~8.0 keV Photon Energy (5th Harmonic)

Undulator: $\lambda_u = 20$ mm, $L_u = 3$ m
 Low-Beta Straight Section of NSLS-II:
 $\beta_x = 1.84$ m ($\sigma_x' = 22$ μ rad at $\epsilon_x = 0.9$ nm)
 $\beta_y = 1.17$ m ($\sigma_y' = 2.6$ μ rad at $\epsilon_y = 8$ pm)

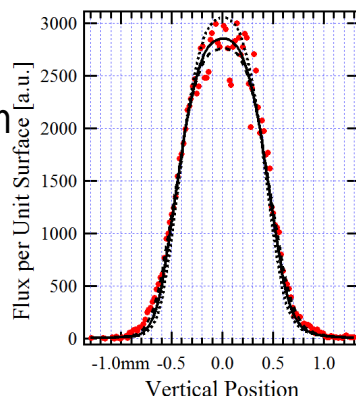


Vertical Cuts Intensity Distributions at 5th Harmonic at Different Undulator Gaps at 30.4 m

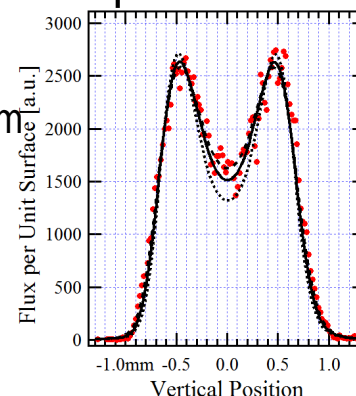
($x = 0$)
 Gap: 5.62 mm



Gap: 5.63 mm

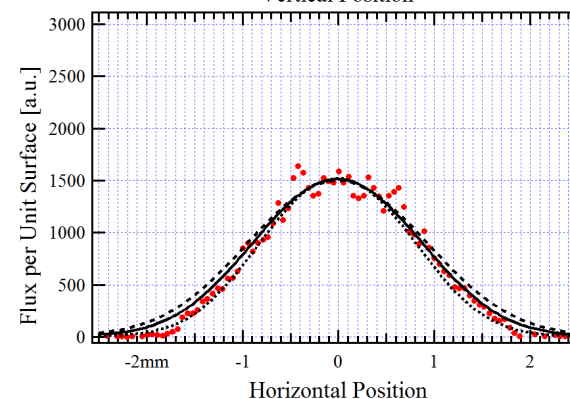
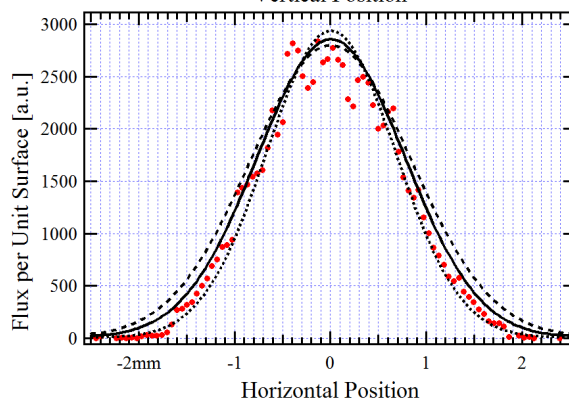
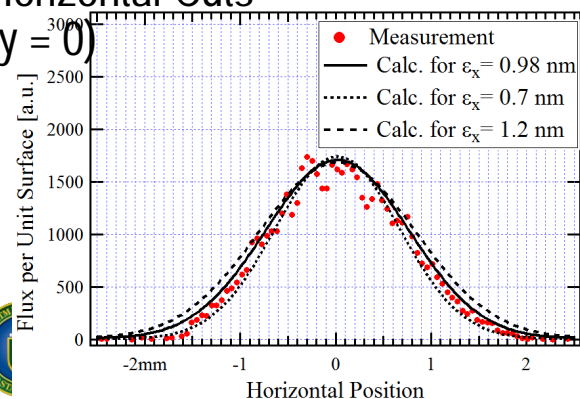


Gap: 5.645 mm



Horizontal Cuts

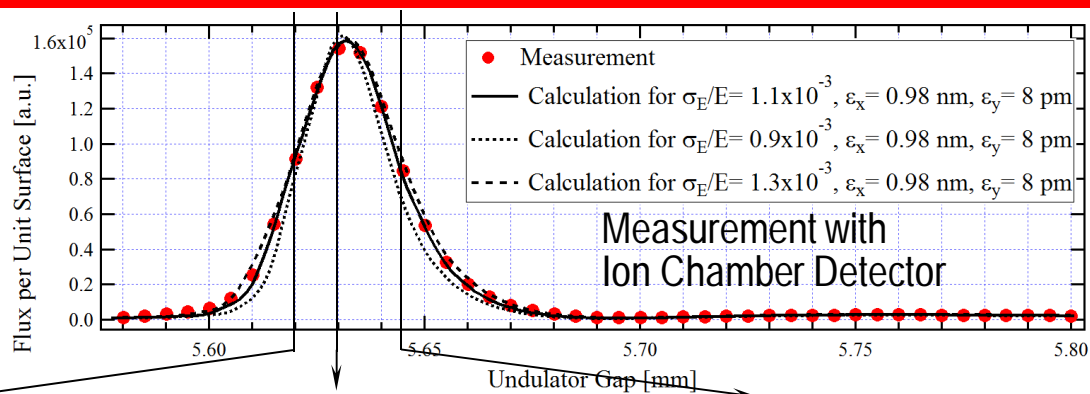
($y = 0$)



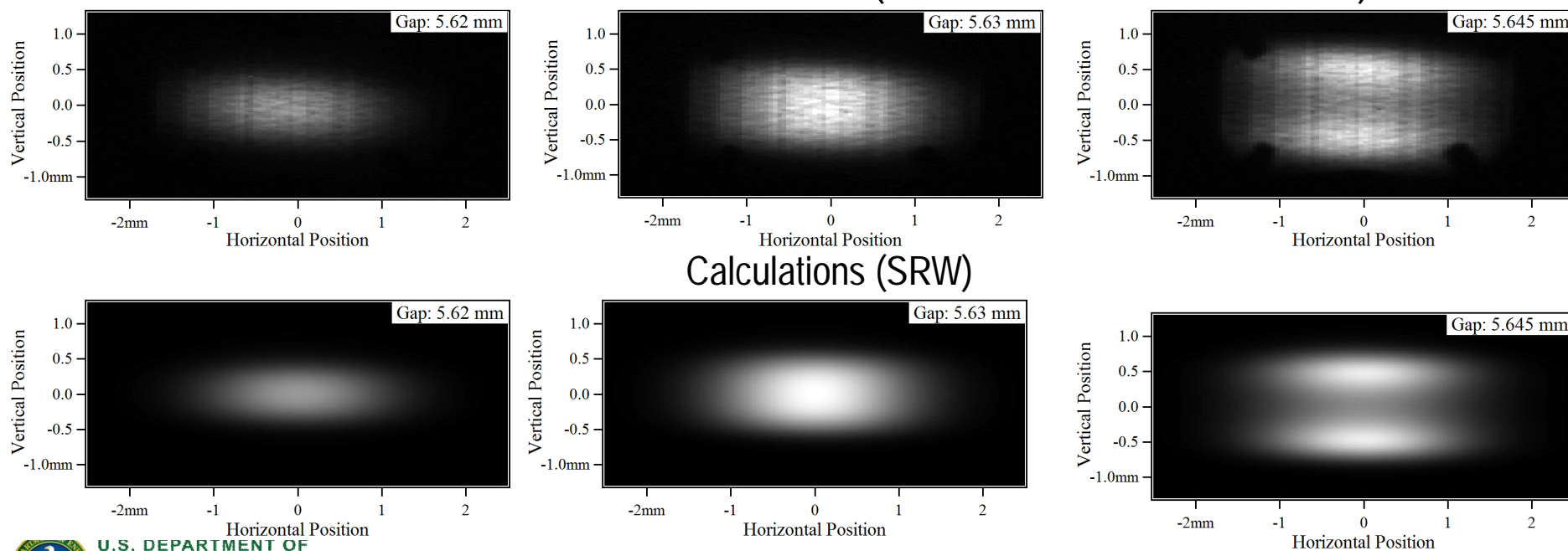
On-Axis "Gap Spectrum" and Intensity Distributions of Radiation from IVU20 at HXN Beamline (II)

On-Axis Gap Spectrum
at ~8.0 keV Photon Energy
(5th Harmonic)

Undulator: $\lambda_u = 20$ mm, $L_u = 3$ m
Low-Beta Straight Section of NSLS-II:
 $\beta_x = 1.84$ m ($\sigma_x' = 22$ μ rad at $\epsilon_x = 0.9$ nm)
 $\beta_y = 1.17$ m ($\sigma_y' = 2.6$ μ rad at $\epsilon_y = 8$ pm)



Intensity Distributions at 5th Harmonic at Different Undulator Gaps at 30.4 m
Measurements after Monochromator (Scintillator Screen + Lens + CCD)



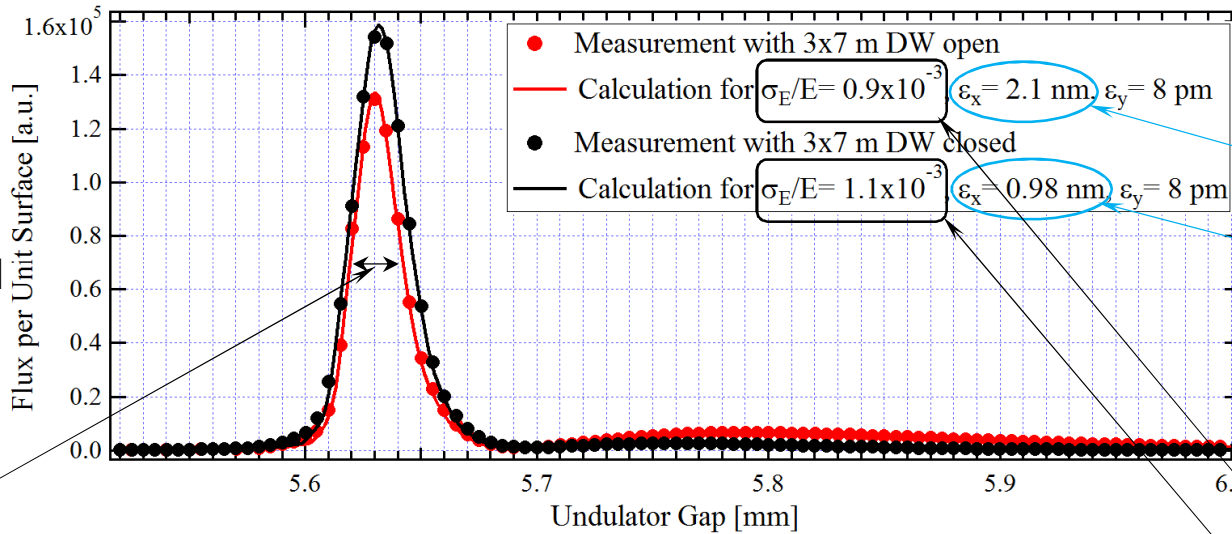
IVU20 (HXN) On-Axis "Gap Spectra" with Damping Wiggler Gaps "Open" and "Closed"

$E_{ph} \approx 8.0$ keV
5th UR Harm.

Low-Beta Straight
Section of NSLS-II
 $\beta_x = 1.84$ m
 $\beta_y = 1.17$ m

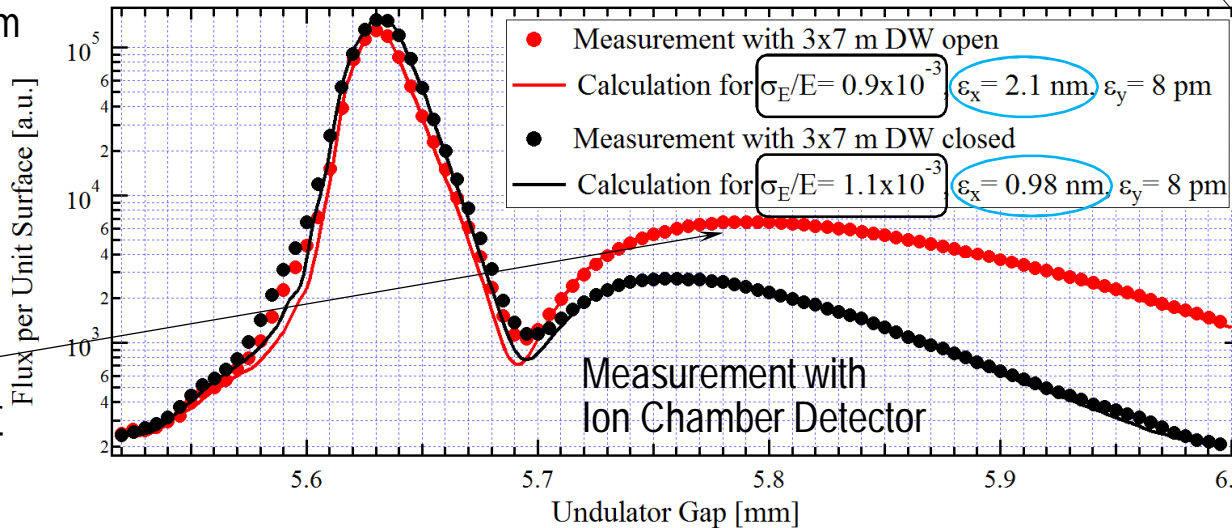
Harmonic width is sensitive to e-beam Energy Spread (and other factors, e.g. undulator field quality)

Intensity in "Side Lobe" is sensitive to e-beam Horizontal Angular Divergence



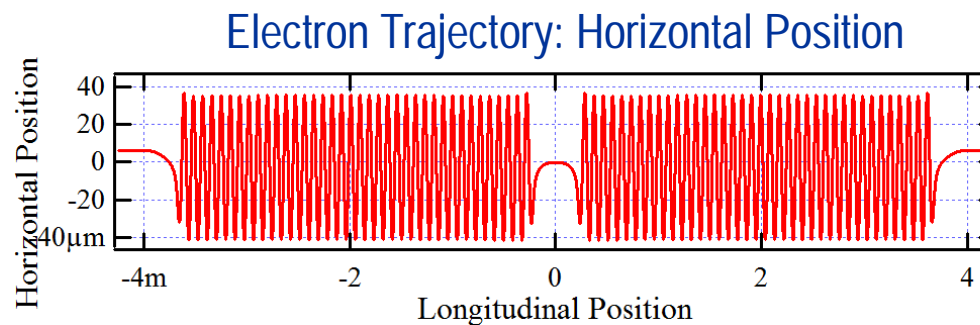
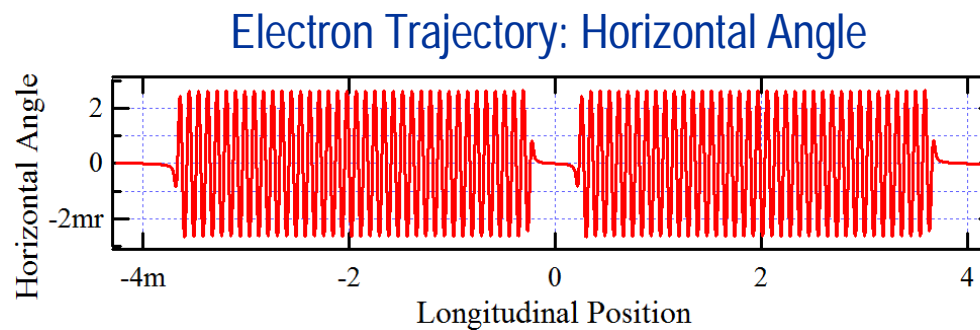
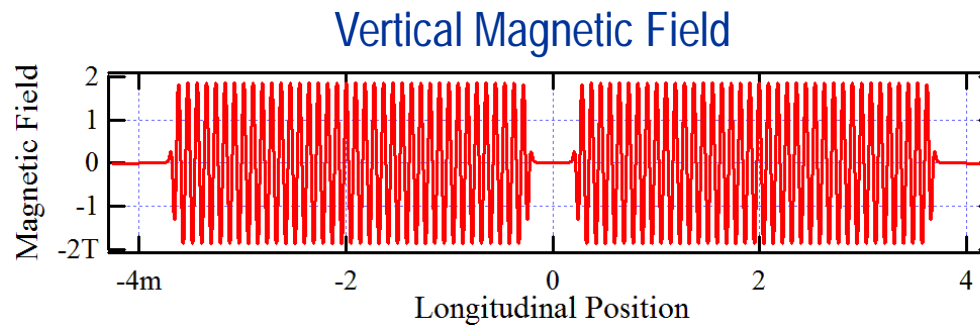
Good Agreement with Accelerator Physics data:
 $\epsilon_x = 2.1$ nm for Bare Lattice,
 $\epsilon_x = 0.9$ nm with 3x7 m DW closed

~Poor Agreement with Accelerator Physics data:
 $\sigma_E/E = 0.5 \times 10^{-3}$ for Bare Lattice,
 $\sigma_E/E = 0.9 \times 10^{-3}$ with 3x7 m DW closed



UR based e-beam diagnostics was used at ESRF (P. Elleaume et al.) and at APS (A. Lumpkin, E. Gluskin et al.)

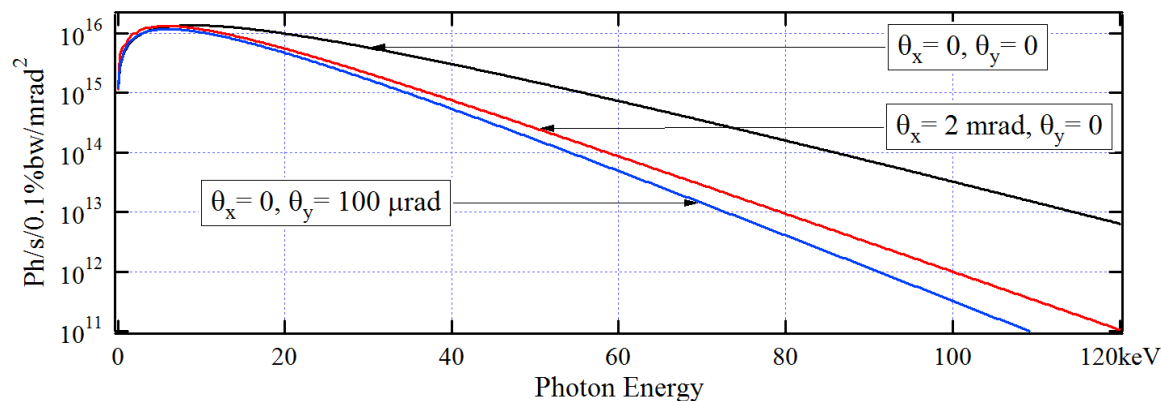
"Inline" Configuration of 2 x 3.5 m Damping Wigglers in High-Beta Straight Section of NSLS-II



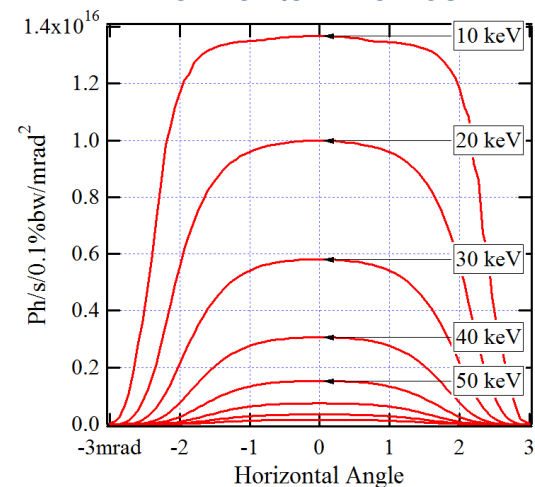
Spectral-Angular Distributions of Emission from 2 x 3.5 m Long Damping Wiggler in "Inline" Configuration

Angular Profiles of DW Emission at Different Photon Energies

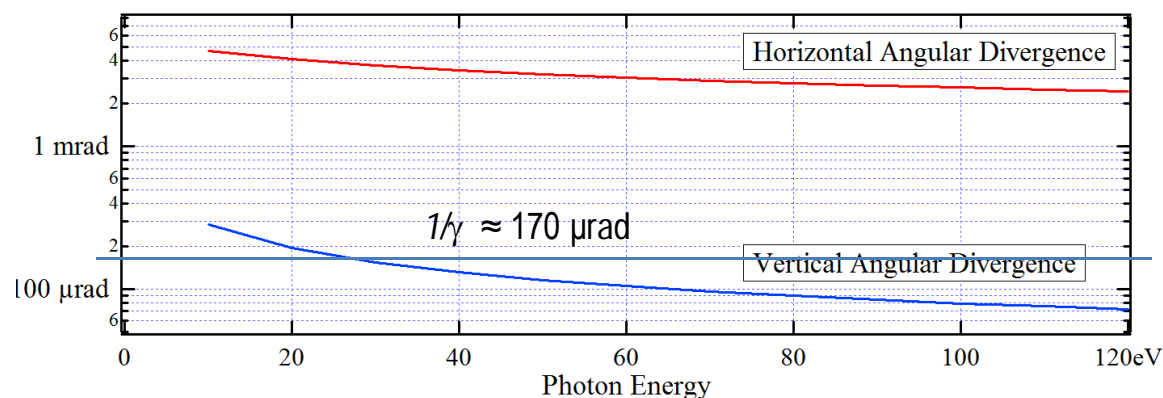
Spectral Flux per Unit Solid Angle



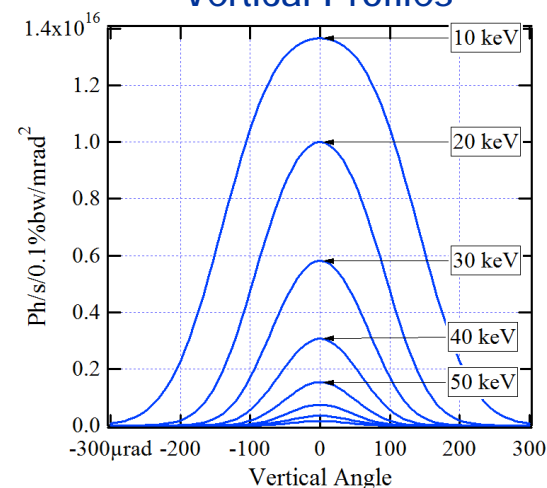
Horizontal Profiles



FWHM Angular Divergence of DW Emission

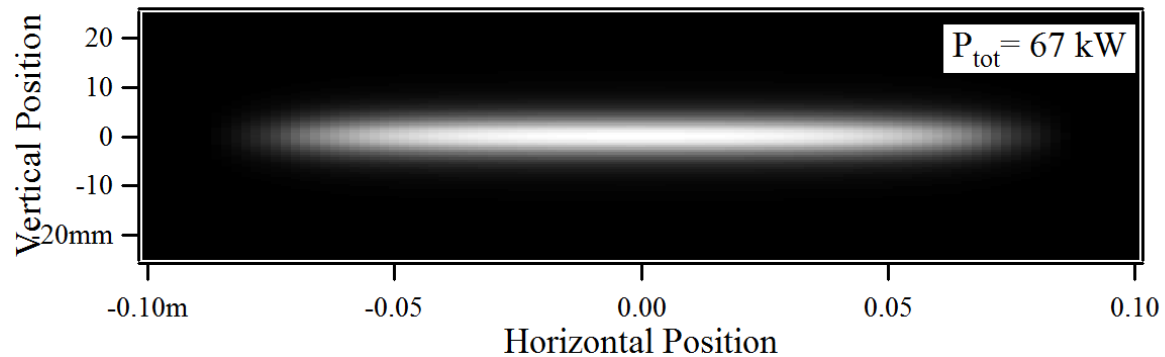


Vertical Profiles

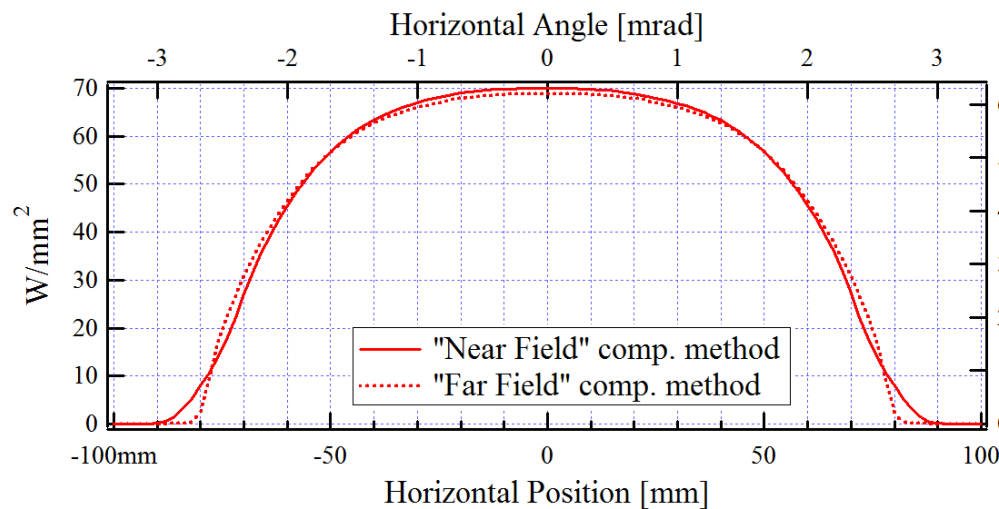


Power Density Distributions of DW90 Emission

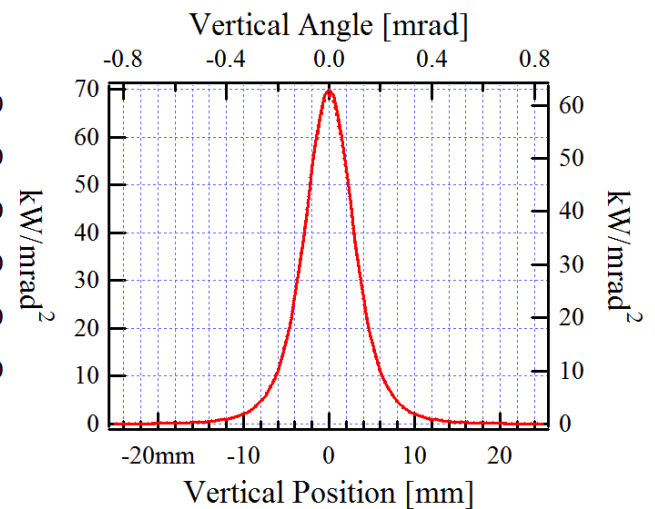
Power Density Distribution in Transverse Plane at 30 m from Center of Straight Section



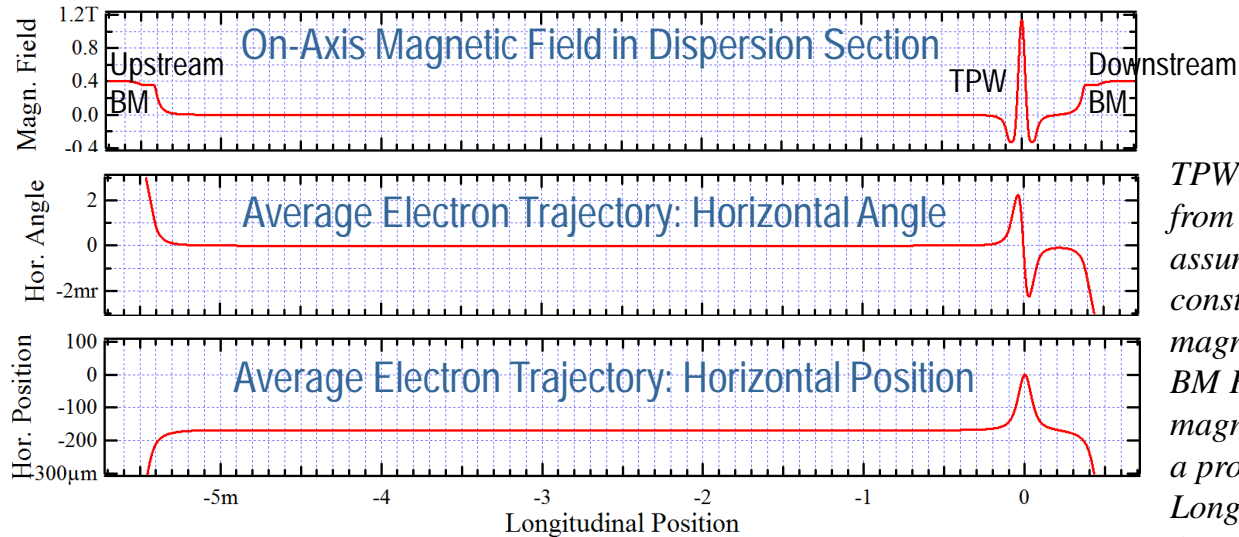
Horizontal Cut ($y = 0$)



Vertical Cut ($x = 0$)

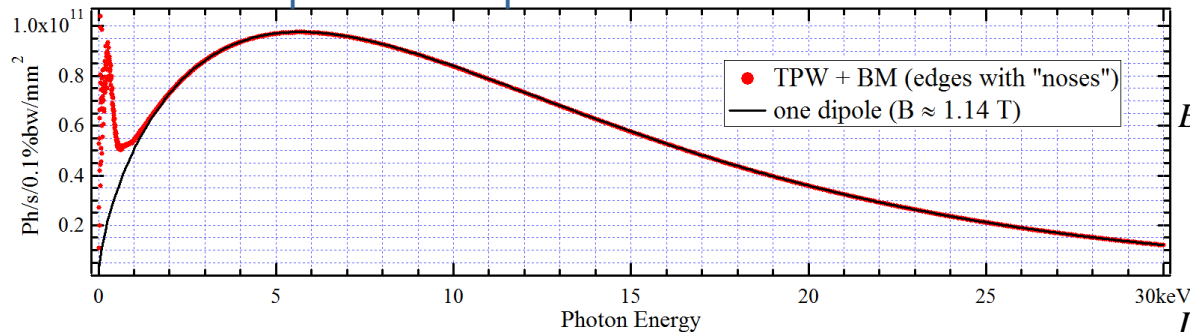


TPW: Magnetic Field, Electron Trajectory and Spectra (in presence of Bending Magnets)



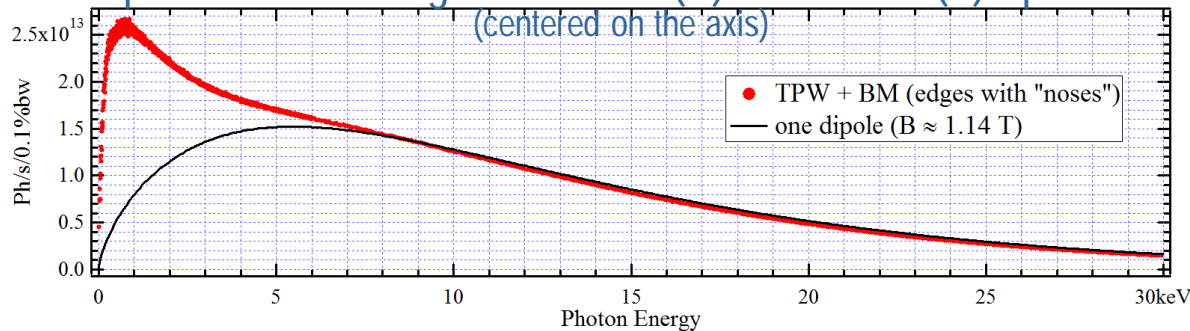
*TPW Field taken from magnetic simulations, assuming that TPW will be constructed out of spare DW magnets;
BM Field is taken from magnetic measurements on a prototype BM with "nose";
Longitudinal Positions are Approximate (+/- 10 cm)*

On-Axis Spectral Flux per Unit Surface at 30 m from TPW



*Electron Energy: 3 GeV
Current: 0.5 A
Hor. Emittance: 0.55 nm
Vert. Emittance: 8 pm*

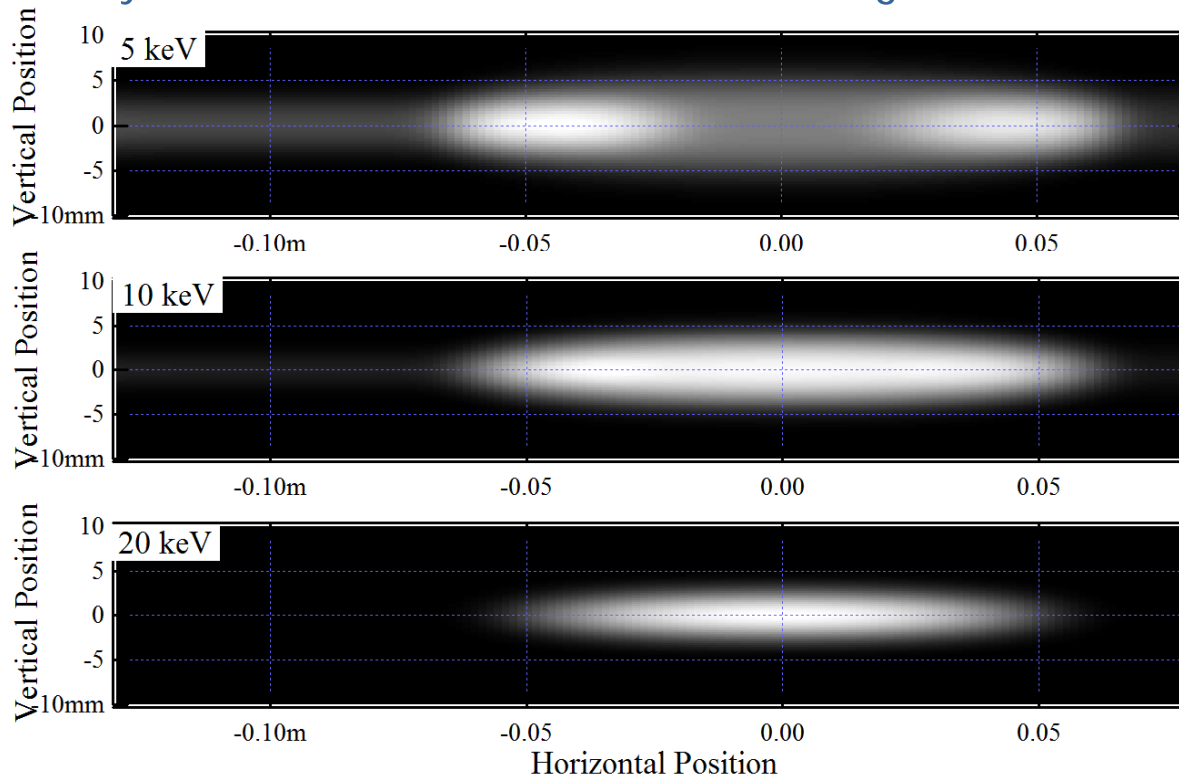
Spectral Flux through 1.75 mrad (H) x 0.1 mrad (V) Aperture (centered on the axis)



*Initial Conditions:
 $\langle x \rangle = 0, \langle x' \rangle = 0$ in TPW
Center*

TPW and BM Radiation Intensity Distributions (Hard X-rays)

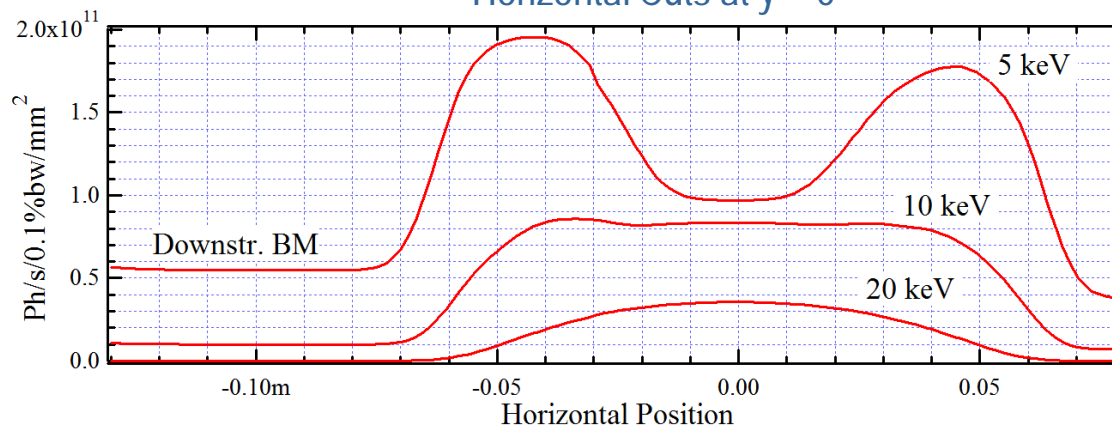
Intensity Distributions at Different Photon Energies at 30 m from TPW



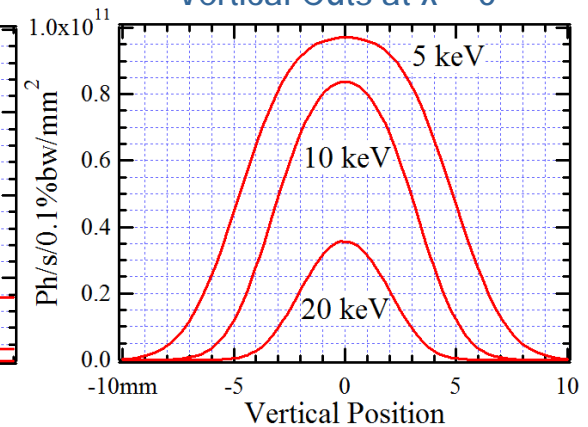
TPW Field taken from magnetic simulations, assuming that TPW will be constructed out of spare DW magnets; BM Field taken from magnetic measurements on a prototype BM with “nose”.

Electron Current: 0.5 A

Horizontal Cuts at $y = 0$

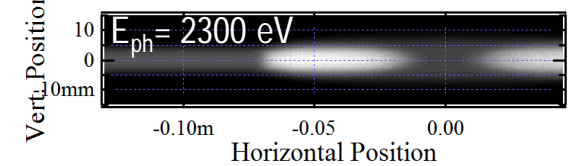
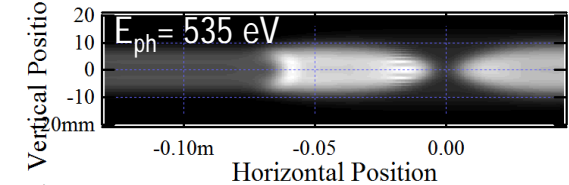
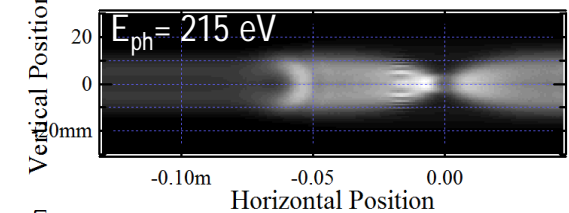
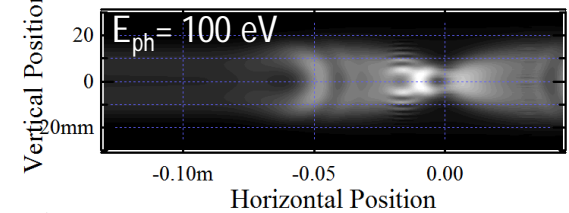
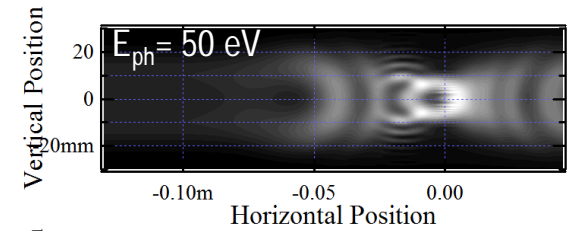
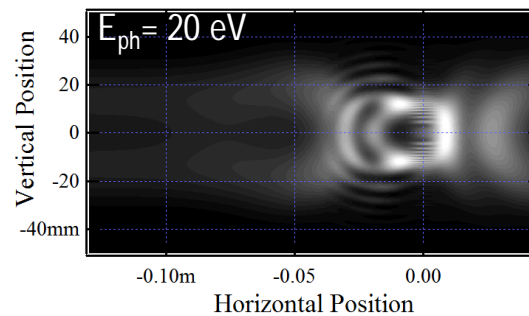
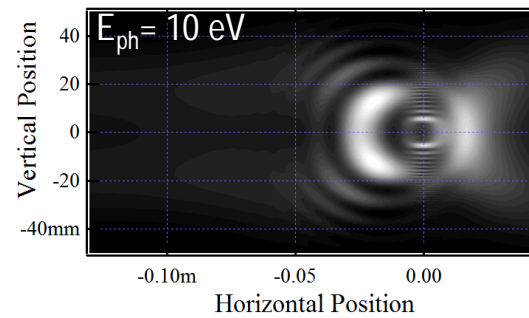
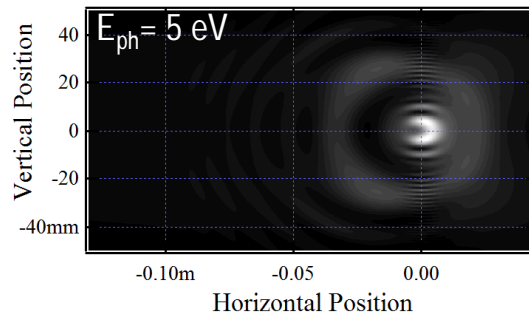
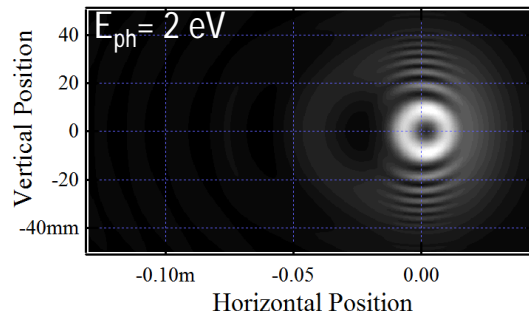
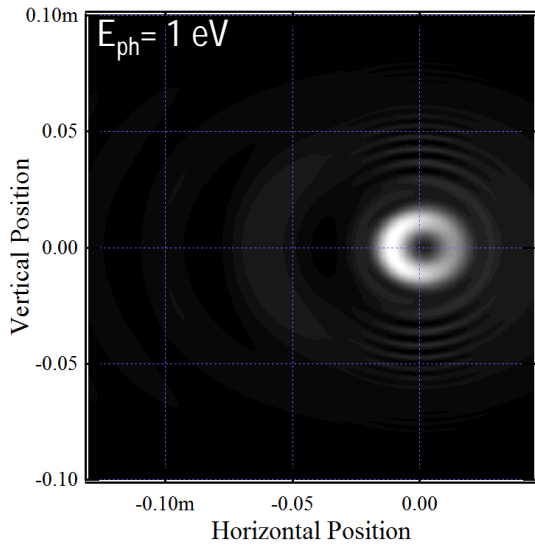
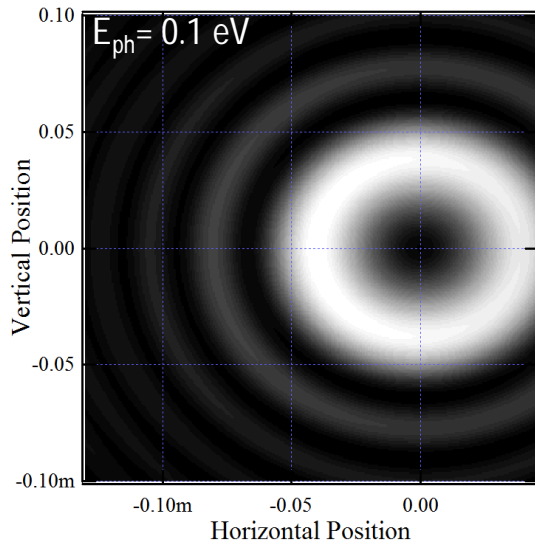


Vertical Cuts at $x = 0$



TPW+BM Radiation Intensity Distributions (IR to Soft X-Rays)

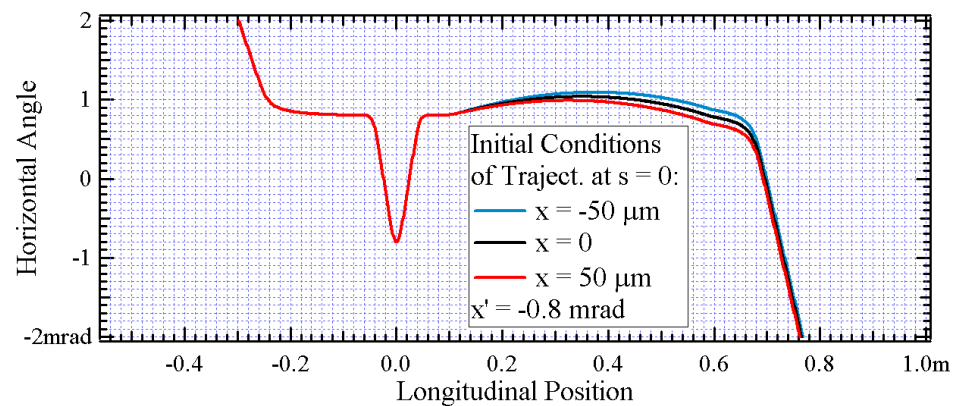
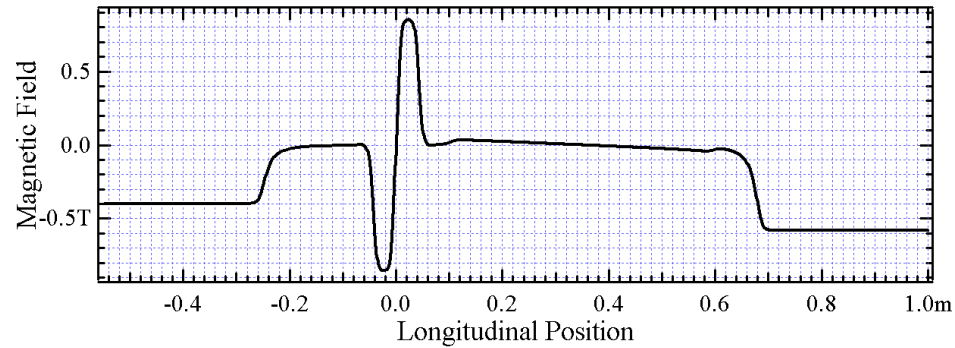
Observation Distance: 30 m
(from TPW center)



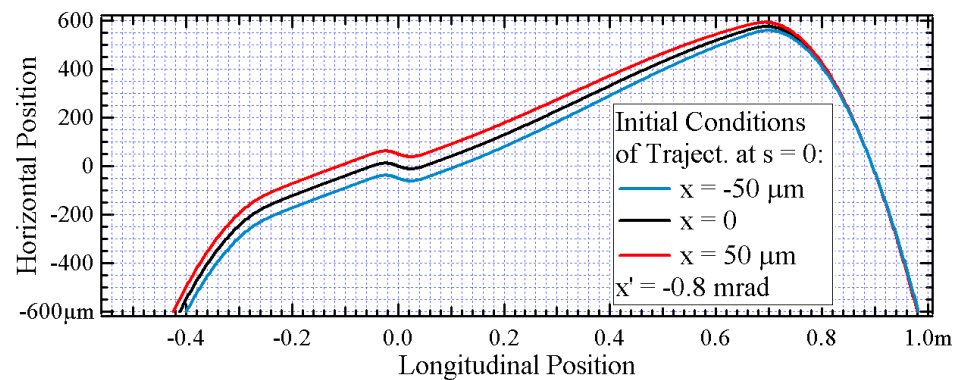
*TPW Field taken from magnetic simulations,
assuming that TPW will be constructed out of
spare DW magnets;
BM Field taken from magnetic measurements
on a prototype BM with “nose”.*

Magnetic Field and Electron Trajectories in ESRF-U 2PW (option)

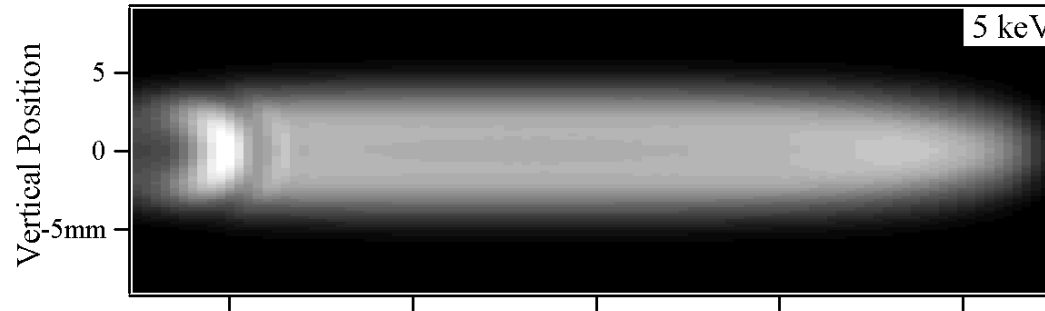
Magnetic Design
by J. Chavanne



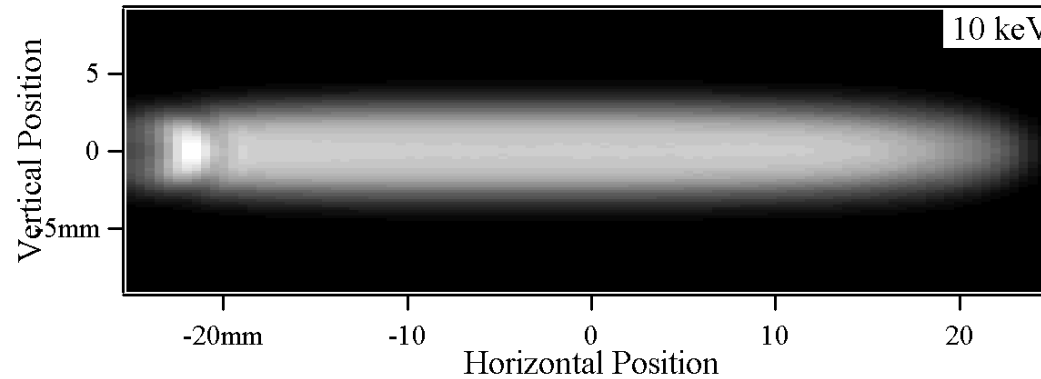
Quadrupole
Lens is included
into analysis
(under testing)



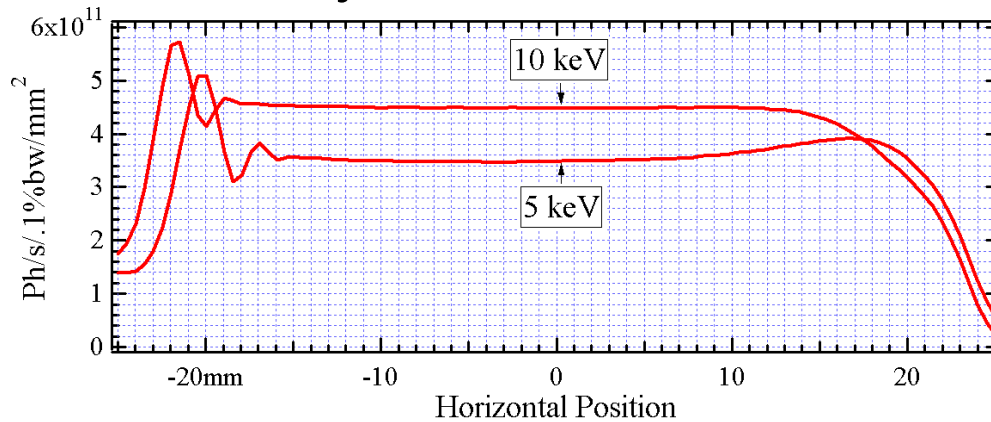
Intensity Distributions of Monochromatic Radiation from ESRF-U 2PW in Projection Geometry



Observation Distance:
 $R = 30$ m



Cuts by Horizontal Median Plane



Cuts by Vertical Plane ($x = 0$)

